Journal of Medicinal Chemistry

Article

pubs.acs.org/jmc

meso-Tetrakis(*p*-sulfonatophenyl)N-Confused Porphyrin Tetrasodium Salt: A Potential Sensitizer for Photodynamic Therapy

Ajesh P. Thomas,[#,‡] P. S. Saneesh Babu,[#,§] S. Asha Nair,[§] S. Ramakrishnan,[⊥] Danaboyina Ramaiah,[⊥] Tavarekere K. Chandrashekar,[‡] A. Srinivasan,*[,‡] and M. Radhakrishna Pillai*[,§]

[‡]National Institute of Science Education and Research (NISER), Bhubaneswar-751005, Orissa, India

[§]Cancer Research Program, Rajiv Gandhi Centre for Biotechnology, Thycaud, Thiruvananthapuram-695014, Kerala, India

[⊥]Photosciences and Photonics Section, Chemical Sciences and Technology Division, National Institute for Interdisciplinary Science and Technology (NIIST-CSIR), Thiruvananthapuram-695019, Kerala, India

Supporting Information

ABSTRACT: A water-soluble derivative of N-confused porphyrin (NCP) was synthesized, and the photodynamic therapeutic (PDT) application was investigated by photophysical and *in vitro* studies. High singlet oxygen quantum yield in water at longer wavelength and promising IC_{50} values in a panel of cancer cell lines ensure the potential candidacy of the sensitizer as a PDT drug. Reactive oxygen species (ROS) generation on PDT in MDA-MB 231 cells and the apoptotic pathway of cell death was illustrated using different techniques.

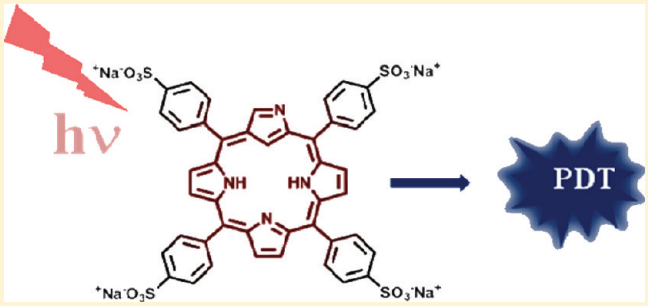

INTRODUCTION

In recent years, photodynamic therapy (PDT) has emerged as a promising and noninvasive treatment for various types of cancer.[1−4] The technique involves controlled generation of short-lived cytotoxic agents within a cell on irradiation of a prodrug or photosensitizer. Light excitation of a dye causes an intermolecular triplet−triplet energy transfer that generates the highly reactive cytotoxic agent, singlet oxygen molecule ($^1O_2$), within a target region, which in turn destroys the affected cells.[5]

PDT application of a sensitizer has coupled with a few specific properties of the photosensitizer such as high absorption coefficient in the red region of visible light, high quantum yield of the triplet state, long triplet state lifetimes, and triplet state of appropriate energy (≥95 kJ mol^{-1}) to allow for efficient energy transfer to ground state oxygen to generate the reactive singlet oxygen species.[6] At the same time, hydrophilicity and specific retention of the sensitizer in the malignant tissues are critical in the successful application of a sensitizer as a photodynamic therapeutic drug.[7,8] Hydrophilicity of the PDT drug ensures better transportation through blood, which in turn can be achieved through sulfonation, carboxylation, or alkylation of N-pyridyl-substituted compounds.[8−11]

In terms of the singlet oxygen quantum yield, dyes, such as rose bengal, rhodamine, hyperacine, eosin, and methylene blue, have proved to be effective photosensitizers, which possess triplet states of appropriate energy for sensitization of oxygen, but lacks practical application in view of other requirements described.[12] On the other hand, porphyrin and its derivatives have been accepted as potent candidates for diverse applications in the areas of biology, medicine, material science, and catalysis.[13] Biocompatibility and preferable absorption in the red region of the analogues such as chlorin, bacteriochlorin, porphyrazine, pheophytin, porphycene, and texaphyrin attained much more importance for their application in photodynamic therapy.[14−17] However, the first photosensitizer approved for clinical use was a mixture of porphyrin derivatives,[18] despite a few drawbacks including its complex structure, relatively low absorption in the tissue transparency window, which diminishes at 630 nm, slow clearance from the body, and prolonged skin photosensitivity.[19] These limitations have been reduced to a certain extent in the second generation of photosensitizers, where compounds with better absorption in the therapeutic window play the role.[14−17]

N-Confused porphyrin, (NCP), an isomer of porphyrin, was introduced independently by Furuta et al.[20] and Latos-Grażyński's group[21] and has a chemical formula of $C_{20}H_{14}N_4$ in its macrocyclic core with an 18 π electron conjugated pathway as a normal derivative. In N-confused porphyrin, one of the pyrrole rings is confused or inverted to form an N3C core with (1.1.1.1) arrangement of *meso*-carbons, and hence it is considered a "true porphyrin isomer". The molecule attained much interest for its versatile receptor properties, coordinates with a vast variety of metal cations, including main group elements,[22−24] lanthanides,[25] and early, middle, and late transition metals,[26−29] and stabilizes their variable oxidation states. Affinities of these derivatives with various anions in the metal complexed form as well as free base state[30] and the biological applications were also explored.[31−33] Interestingly, the better

Received: January 3, 2012
Published: May 14, 2012

dx.doi.org/10.1021/jm300009q | *J. Med. Chem.* 2012, 55, 5110−5120

Scheme 1. Synthesis of NCPS

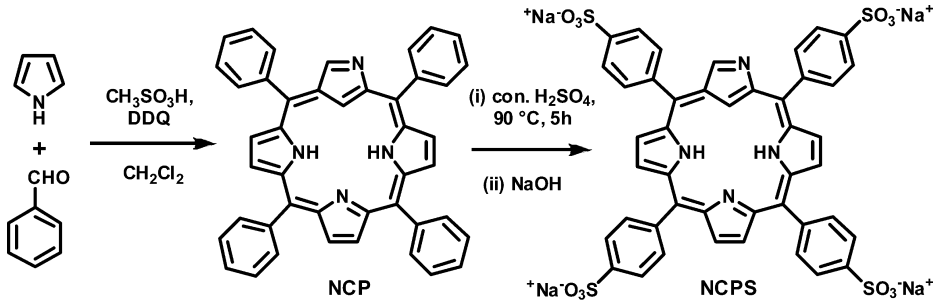

molar extinction coefficients compared with normal porphyrin in the higher Q-band region may suit the confused derivatives as a sensitizer for PDT. Even though the N-confused porphyrin derivatives are well-known for their receptor properties,[22−30] reports in which these derivatives are used in PDT applications are rare. Here in this report, we introduce a water-soluble derivative of N-confused porphyrin, *meso*-tetrakis(*p*-sulfonatophenyl)-N-confused porphyrin tetrasodium salt (NCPS) and investigate the photodynamic activity of the sensitizer by photophysical studies in water as well as in methanol and *in vitro* analysis with different cancer cells lines.

RESULT AND DISCUSSION

The synthesis of *meso*-tetrakis(*p*-sulfonatophenyl)N-confused porphyrin tetrasodium salt (NCPS) involves a two-step process as shown in Scheme 1, starting from tetraphenyl N-confused porphyrin (NCP), which was prepared by Lindsey's method.[34] To synthesize NCPS, we adopted the known method of sulfonation for normal porphyrin,[35] where the tetraphenyl derivative was dissolved in concentrated H_2SO_4 and heated for 5 h at 90 °C, then stirred overnight at room temperature. After neutralization of the excess acid with sodium hydroxide solution, the reaction mixture was washed many times with methanol to extract the compound and filtered to remove the sodium sulfate salt formed during neutralization. The methanol solution was evaporated, and the solid obtained was extracted through a Soxhlet apparatus using methanol to derive NCPS in 56% yield from the corresponding tetraphenyl derivative. The compound was highly soluble in water and characterized by using ^{1}H NMR, ^{13}C NMR, MALDI-TOF, and IR analysis.[36]

Electronic Absorption and Photophysical Properties. Absorption spectra of the compound (Figure 1) were recorded both in deionized water and in methanol and showed the Soret band at 444 and 440 nm, respectively, with Q-bands ranging from 550 to 800 nm. The better absorption of NCPS compared with the counterpart of normal porphyrin after 700 nm (1400 M^{-1} cm^{-1} at 747 nm in water for NCPS, where the absorbance of normal sulfonated derivative ends at 630 nm) enhances the utility of the sensitizer as a photodynamic therapeutic drug. On the other hand, the fluorescence quantum yield calculated for NCPS with respect to tetraphenyl porphyrin was too low, and the yield obtained in methanol is 0.0032,[36] which is comparable with the similar N-confused systems.[37]

Triplet−triplet energy transfer is the key step to generate singlet oxygen, which is the cytotoxic agent in photodynamic therapy. Hence a stable triplet state and efficient energy transfer enhances the possibility of a photosensitizer to be used as a photodynamic therapeutic drug, and the quantification of these parameters are in terms of triplet lifetime and triplet quantum yield, respectively. Triplet state properties of N-confused

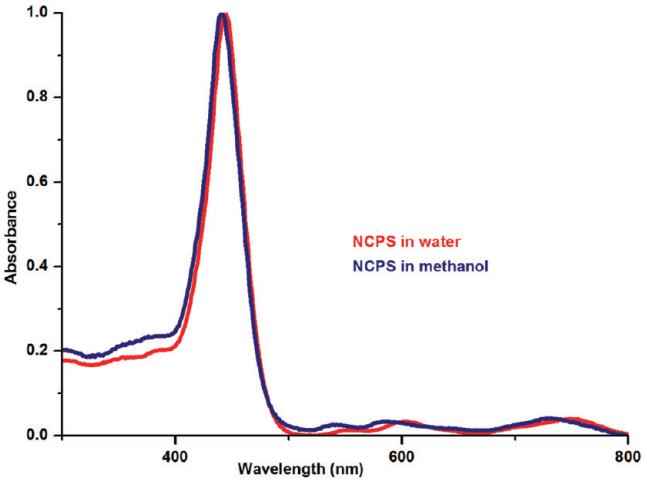

Figure 1. Normalized absorption spectra of NCPS both in methanol and deionized water.

porphyrins are well studied in the literature.[38−40] Transient state properties of NCPS were investigated using nanosecond laser flash photolysis with a 355 nm laser pulse. Figure 2 shows the triplet absorption of NCPS in deionized water with the decay profile at 490 nm in the inset. The formation of the triplet state was confirmed by the absorption quenching in the presence of dissolved oxygen.[36] Transient absorption of the compound

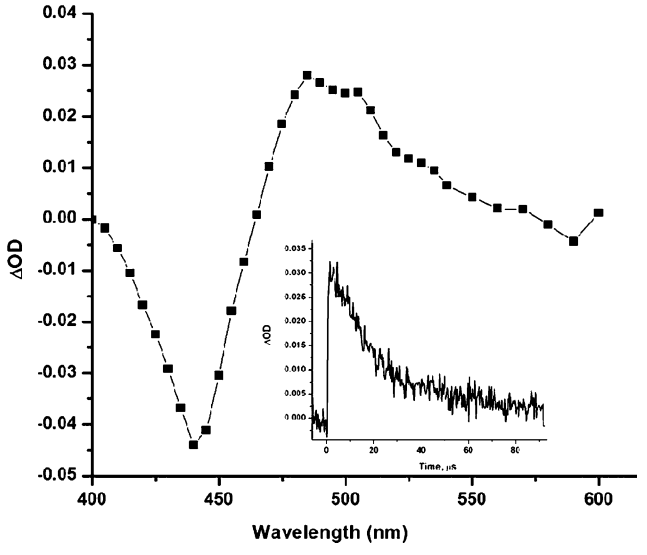

Figure 2. Triplet absorption of NCPS in deionized water recorded at 7.2 μs. Inset shows the transient decay at 490 nm.

dx.doi.org/10.1021/jm300009q | J. Med. Chem. 2012, 55, 5110−5120

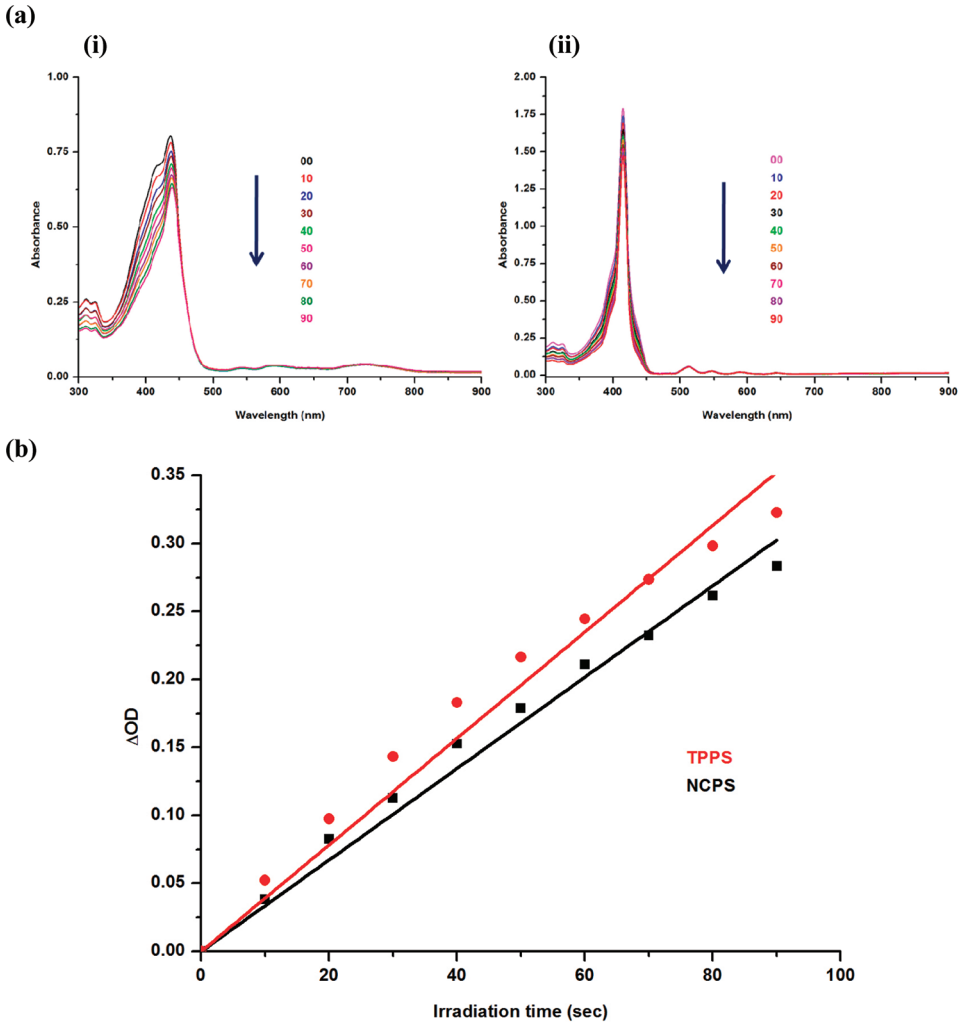

Figure 3. (a) Change in the absorption spectra of DPBF upon irradiation with (i) NCPS or (ii) TPPS in methanol and (b) Plot of change in absorbance of DPBF at 411 nm vs irradiation time (λ_{irr} > 600 nm) in the presence of NCPS versus TPPS as the standard in methanol.

shows maxima at 490 nm in deionized water with bleach at 440 nm range where the compound has significant ground state absorption. Triplet absorption profile of the compound in methanol was similar to that in water.[36] Triplet lifetime of the compound was measured both in deionized water and in methanol and found to be 16 and 1.2 μs, respectively.[36] Since, low water solubility and triplet lifetime remain the main barriers for many sensitizers to their real application, comparatively better triplet lifetime of the sensitizer in water was promising.

The efficiency of triplet−triplet energy transfer was quantified by calculating triplet quantum yield, using the energy transfer method to β-carotene with tris(bipyridyl)ruthenium(II) complex, $[Ru(bpy)_3]^{+2}$.[41,42] However, the insolubility of β-carotene in water prevents determination of the triplet quantum yield of the sensitizer in water, but the respective value in methanol was obtained as 0.70 ± 0.05.

The generation of cytotoxic singlet oxygen from its triplet ground state by the energy transfer process from the triplet state of the sensitizer underscores an important step in photodynamic therapy. We adopted an indirect method to calculate the singlet oxygen quantum yield using 1,3-diphenyl isobenzofuran (DPBF) as a singlet oxygen scavenger[43−45] and *meso*-tetrakis(*p*-sulfonatophenyl)porphyrin tetrasodium salt (TPPS) as reference, where the singlet oxygen quantum yield of TPPS was found to be 0.60 in water and 0.70 in alcohols.[46,47] In order to calculate the quantum yield, the sensitizer along with DPBF was irradiated using a xenon lamp with a 600 nm long pass filter at different time intervals from 10 to 90 s. The decrease in the absorption of DPBF was monitored at 411 nm as shown in Figure 3a, which is due to the dye sensitized generation of singlet oxygen followed by photooxidation of DPBF. Absorbance at the irradiating wavelength was adjusted to 0.02 for both the sensitizer and the reference. From the slope of the graph obtained by plotting change in optical density against the time interval (Figure 3b), the singlet oxygen quantum yield was calculated as 0.70 ± 0.03 in methanol and 0.55 ± 0.05 in water.[36]

***In Vitro* Studies.** *Cytotoxicity Studies of NCPS in Different Cell Lines.* Photocytotoxicity of sulfonated derivatives of different porphyrin and phthalocyanine derivatives have been studied extensively during the past years. These sulfonated derivatives were known for their excellent membrane permeability and lysosomal accumulation in cells with high selectivity toward carcinomas.[48−50] The photodynamic activity of NCPS was evaluated against eight different cell lines, namely, human colon cancer cells (HCT-116), human breast cancer cells (MCF7-ER, PR positive, and MDA-MB-231-ER, PR negative), human pancreatic cancer cells (MIA-PaCa-2), human cervical cancer cells (HeLa and SiHa), and human oral cancer cells (SCC-172 and SCC-131).

dx.doi.org/10.1021/jm300009q | *J. Med. Chem.* 2012, 55, 5110−5120

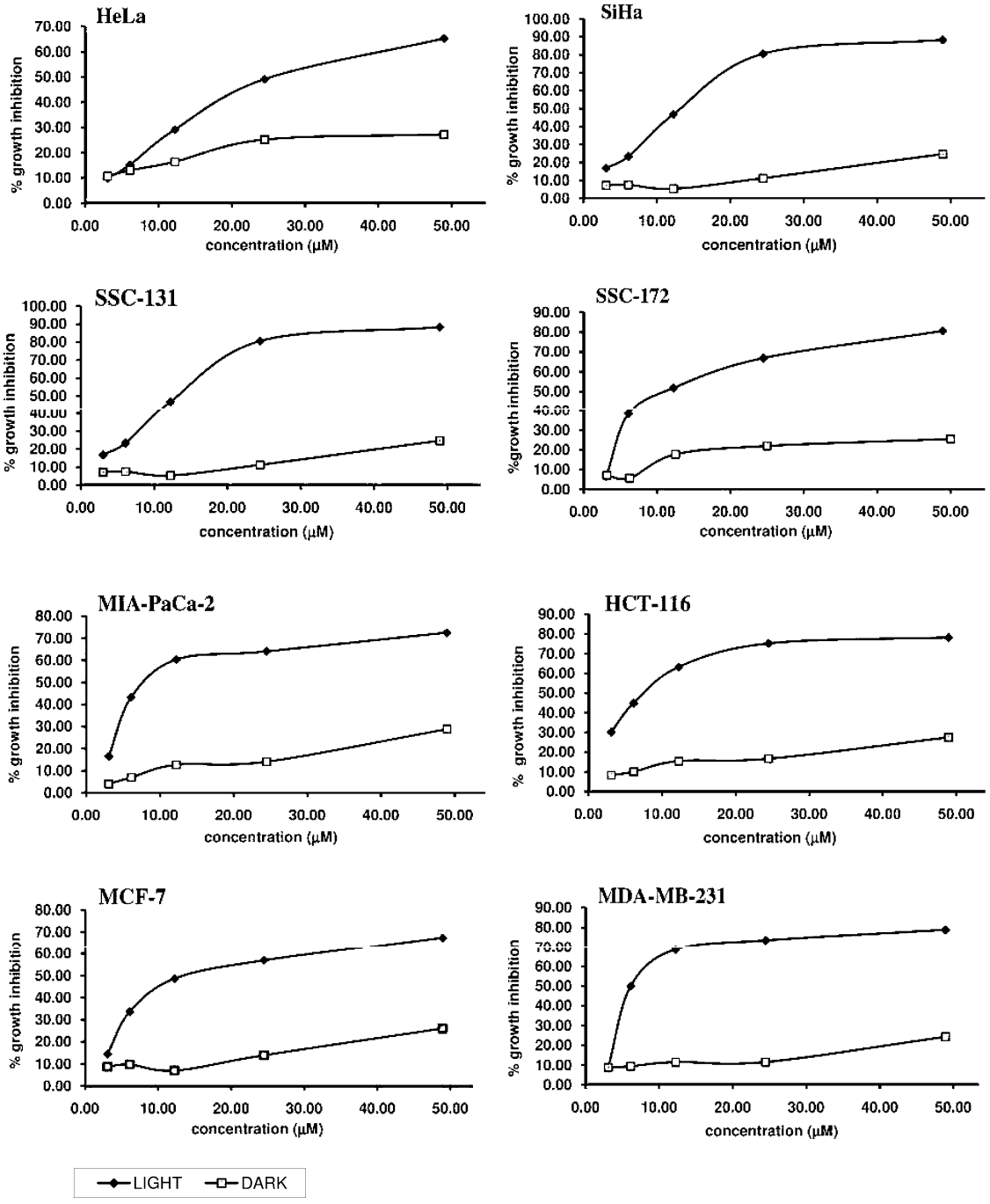

Figure 4. MTT assay was done on a panel of cancer cells and shows cytotoxicity of NCPS in the presence and absence of light. NCPS shows significant cytotoxicity in the presence of light in all cells but shows negligible cytotoxicity in the absence of light.

The cytotoxicity of NCPS in these cell lines was investigated both in the presence and in the absence of light using MTT assay as shown in Figure 4.

Cytotoxic studies revealed that NCPS is essentially non-cytotoxic in the absence of light but interestingly on the other hand exhibits high photocytotoxicity. The comparative study of IC_{50} values for NCPS on the above cell lines showed that the IC_{50} value of MDA-MB-231 cells (6 μM) is about 5-fold lower than that for the HeLa cells (25 μM). Oral and cervical cancer cells showed an increase in IC_{50} values compared with breast, pancreatic, and colon cancer cells (Table 1). Our observations suggest that NCPS exhibits more photocytotoxicity toward adenocarcinomas over the other epithelial cancer cell lines studied.

NCPS-Sensitized ROS Generation. Reactive oxygen species (ROS), particularly singlet oxygen, have a central role in photodynamic cytotoxicity.[51−54] During our investigation, the formation of cellular ROS after PDT with NCPS was determined using the CM-H2DCFDA probe (Invitrogen). The probe emits a green fluorescence after the oxidation reaction with reactive oxygen species and after the diacetate groups are removed by cellular esterase.[55,56] NCPS induced accumulation of ROS in the cells, resulting in a substantial increase in the number of fluorescent cells as detected by flow cytometry and fluorescent imaging. MDA-MB-231 cells showed the least IC_{50} value (6 μM);

dx.doi.org/10.1021/jm300009q | J. Med. Chem. 2012, 55, 5110−5120

Table 1. Comparison of IC_{50} Values of NCPS in a Panel of Cancer Cells

cell line	IC_{50} (μM)
HeLa	25
SiHa	20
SCC-131	13
SCC-172	11
MIA-PaCa-2	8
HCT-116	8
MCF-7	12
MDA-MB-231	6

hence for further investigation this cell line formed the model for analysis. Figure 5 shows the effects of NCPS on ROS generation followed by PDT and the concentration-dependent increase in cellular ROS content after PDT with NCPS.

Cellular damage during photodynamic therapy is mediated through apoptosis.[57] Apoptosis is a normal physiological process essential for the control of tissue development, involution, and tissue homeostasis.[58] It is a tightly regulated process of cell suicide, controlled by both intracellular and extracellular signals, terminating in a characteristic sequence of morphological and biochemical changes for the systematic dismantling of the cell. The process limits leakage of intracellular material to the immediate environment and thereby prevents tissue inflammation.[59]

The earliest hallmark of apoptosis is the loss of plasma membrane asymmetry.[45] In apoptotic cells, the membrane phospholipid phosphatidylserine is translocated from the inner to outer leaflet of the plasma membrane, thus exposing phosphatidylserine to the external cellular environment. Annexin V (tagged with FITC) has high affinity for phosphatidylserine and therefore serves as a sensitive probe for identifying apoptotic cells by fluorescence microscopy and flow cytometry.[60]

Generally, Annexin V−FITC is used together with propidium iodide (PI), which is another fluorescent probe to distinguish viable cells from dead cells, because the former can penetrate through the intact and viable cells but the latter only dead cells. We studied the cell death mechanism induced by PDT using NCPS by examining the dual fluorescence of Annexin V−FITC/PI using flowcytometry as shown in Figure 6. The cell populations at different phases of cell death, namely, viable (AnnexinV−$FITC^-/PI^-$), early apoptotic (Annexin V−$FITC^+/PI^-$), and necrotic or late-stage apoptotic (Annexin V−$FITC^+/PI^+$) were examined at different drug doses.

We observed that most of the cells were negative for Annexin V−FITC and PI after treatment with NCPS (12 μM) in the absence of light. This indicates that NCPS is noncytotoxic toward MDA-MB-231 cells in darkness. However, upon illumination, the percentage of cells at the early apoptotic stage (i.e., externalization of phospholipid phosphatidylserine but not membrane leakage, Annexin V−$FITC^+/PI^-$) increased from 3.5% ± 0.41% to 83.9% ± 7.8% when the concentration of NCPS increased from 0 to 12 μM. From these results, it can be concluded that NCPS upon PDT induces apoptosis extensively.

Chromatin condensation is another sensitive marker of apoptosis,[61−63]along with a decrease in membrane potential across the mitochondrial inner membrane.[64,65] In the present study, Hoechst stain was employed to observe chromatin condensation, and cells were viewed under a fluorescent microscope. It was found that PDT with NCPS in MDA-MB-231 cells at 6 μM resulted in 72% ± 4.6% chromatin condensation, whereas at 12 μM 91% ± 2.6% condensation was observed. In light and dark controls, only 10.4% ± 1.5% and 7.6% ± 1.2% chromatin condensation was observed (Figure 7). This demonstrates that NCPS induces apoptosis in a concentration-dependent manner.

Also, the changes in mitochondrial membrane potential were monitored using the JC1 cationic fluorescent dye. The accumulation of JC1 in mitochondria yields both green and red fluorescence. However, a decrease in the mitochondrial inner membrane potential due to apoptosis causes a decrease in red fluorescence that can be easily monitored by fluorescent microscopy.[66−68] PDT with NCPS in MDA-MB-231 cells at 6 μM resulted in about 69.7% ± 5.4% decrease in membrane potential, where as at 12 μM, 88.5% ± 4.9% decrease in mitochondrial membrane potential was observed. In light and dark controls, only 12.1% ± 4.9% and 10.3% ± 1.3% chromatin condensation was observed (Figure 7). Thereby our studies illustrate a mitochondrial-mediated cell death pathway through apoptosis during PDT with NCPS.

Another confirmation for NCPS-induced apoptosis was from the cleavage of PARP, a 116 kDa nuclear poly(ADP-ribose) polymerase, which is involved in DNA repair reaction to cellular stress.[69] This protein can be cleaved by many ICE-like caspases *in vitro*[70,71] and is one of the main cleavage targets of caspase-3 *in vivo*.[72,73] In human PARP, the cleavage occurs between Asp214 and Gly215, which separates the PARP amino-terminal DNA binding domain (24 kDa) from the carboxy-terminal catalytic domain (89 kDa).[70−72] PARP helps cells to maintain their viability; cleavage of PARP facilitates cellular disassembly and serves as a marker of cells undergoing apoptosis.[74] During our experiment, no PARP cleavage was observed after treatment with NCPS (12 μM) in the absence of light, which again confirms the noncytotoxic nature of NCPS in the absence of light (Figure 8). However, upon illumination, NCPS induces PARP cleavage at both concentrations of 6 and 12 μM, thus confirming that NCPS induces cell death via apoptosis.

CONCLUSION

In conclusion, a water-soluble N-confused porphyrin derivative with better molar extinction coefficient in the red region of visible light compared with normal porphyrin derivatives has been synthesized. Photophysical studies of the molecule have been conducted both in deionized water and in methanol followed by *in vitro* anticancer studies. The calculated value of singlet oxygen quantum yield of the sensitizer was comparable with the reported value of other structurally similar porphyrin derivatives. *In vitro* studies analyzed in a series of cancer cell lines showed promising IC_{50} values. Upon illumination, NCPS exhibited more photocytotoxicity to adenocarcinomas than the other epithelial cell lines, and maximum activity has been attributed toward breast adenocarcinoma MDA-MB-231 cells, with an IC_{50} value as low as 6 μM. As shown by flow cytometry and fluorescent imaging using ROS probe CM-H2DCFDA, NCPS induces accumulation of ROS in the cells in a concentration-dependent manner. Apoptosis-induced cell death during PDT with NCPS was found to be mediated in a mitochondrial-dependent manner as evidenced by JC1 mitochondrial membrane potential assay. Apoptotic potential of NCPS was also confirmed by DNA condensation, Annexin V apoptotic assay, and PARP cleavage. Overall, both the photophysical and *in vitro* studies ensure the potential candidacy of the sensitizer as a photodynamic therapeutic drug, and *in vivo* analysis is underway in our laboratory.

dx.doi.org/10.1021/jm300009q | *J. Med. Chem.* 2012, 55, 5110−5120

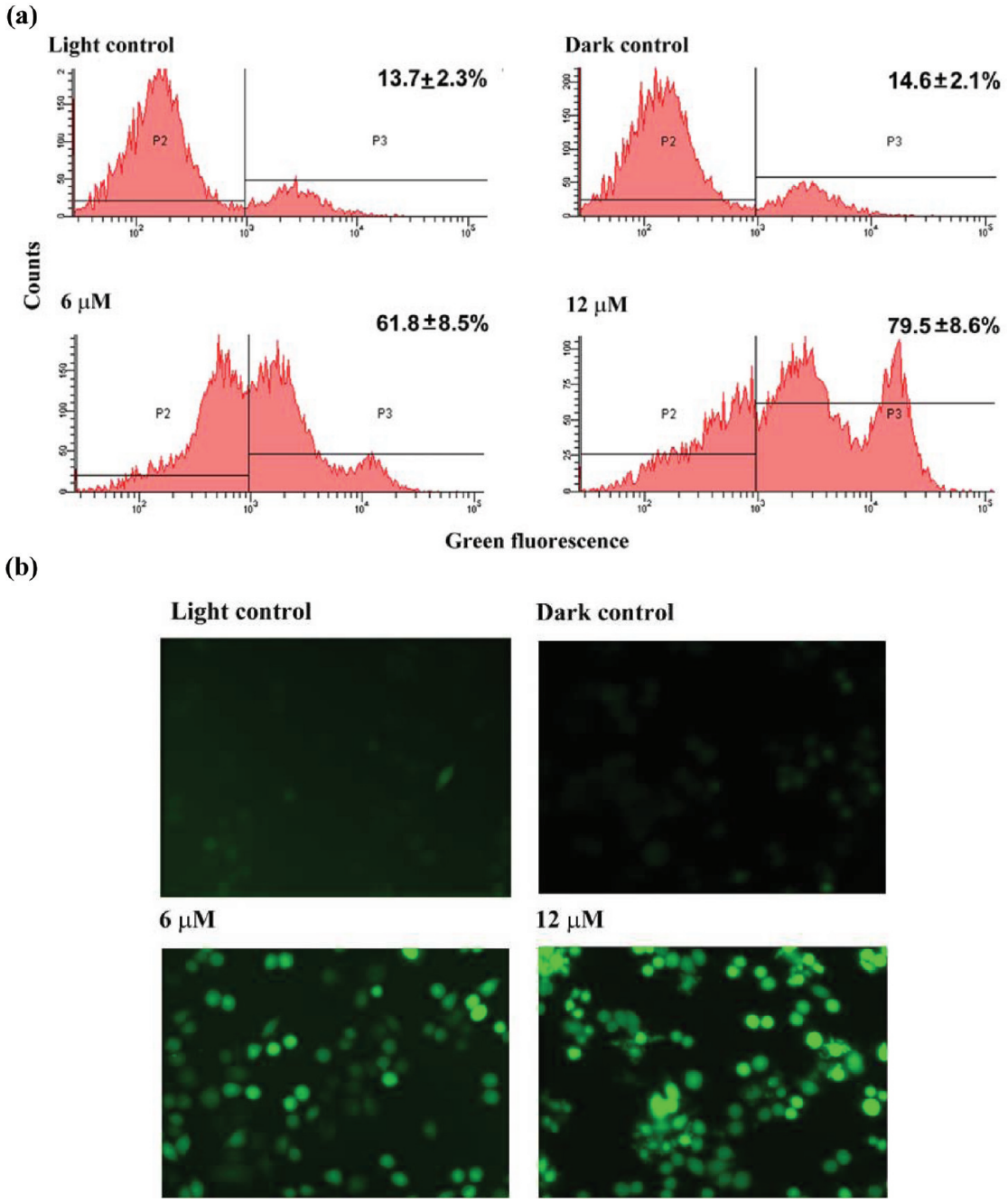

Figure 5. NCPS (12 μM)-treated cells in the dark (dark control) and without NCPS in light (light control) were then labeled with the CM-H2DCFDA probe after 24 h of PDT. (a) Flow cytometry analysis of MDA-MB-231 cells, showing induction of intracellular ROS by NCPS in PDT. Data are expressed as a mean value ± standard deviation of three independent experiments. Here the population P2 shows background fluorescence, which represents cells with low ROS, and the population P3 shows cells with enhanced fluorescence indicating cells with high ROS. Here we observed an increase in P3 population from 13.7% ± 2.3% to 79.5% ± 8.6% when concentration of NCPS increased from 0 to 12 μM. (b) Fluorescence images of MDA-MB-231 cells shows enhanced fluorescence after PDT with 6 and 12 μM NCPS.

EXPERIMENTAL SECTION

Materials and Methods. Tetrasulfonated derivative of N-confused porphyrin (NCPS) was prepared from corresponding tetraphenyl N-confused porphyrin, which in turn was prepared by Lindsey's method.[34] The reagents for the synthesis as well as photophysical studies were obtained from Sigma-Aldrich and Merck, India, and used as such. All solvents were distilled and dried before use. Deionized water was from Millipore.

^{1}H and ^{13}C NMR spectra were recorded on a Bruker Biospin 400 MHz spectrometer. NMR experiments were done in DMSO-d_6. ^{1}H NMR spectra were obtained in 512 scans and ^{13}C in 17000 scans. Spectra were referenced internally by using the residual solvent (^{1}H δ = 2.5 and ^{13}C δ = 39.4 for DMSO-d_6) resonances relative to $SiMe_4$. Matrix-assisted laser desorption ionization−time-of-flight (MALDI−TOF) mass spectra were recorded in a Shimadzu Biotech Axima mass spectrometer. Elemental analysis were conducted using a Perkin-Elmer 2400 series II instrument, and the purity of the compound was determined as >95%. Infrared spectrum of the compound was recorded on a Perkin-Elmer FT-IR spectrometer, spectrum RXI.

Electronic absorption spectra and steady-state fluorescence spectra were recorded on an Agilent diode array UV−visible spectrophotometer (model 8453) and Perkin-Elmer LS55 fluorescence spectrometer, respectively. The transient absorption studies were carried out using

dx.doi.org/10.1021/jm300009q | J. Med. Chem. 2012, 55, 5110−5120

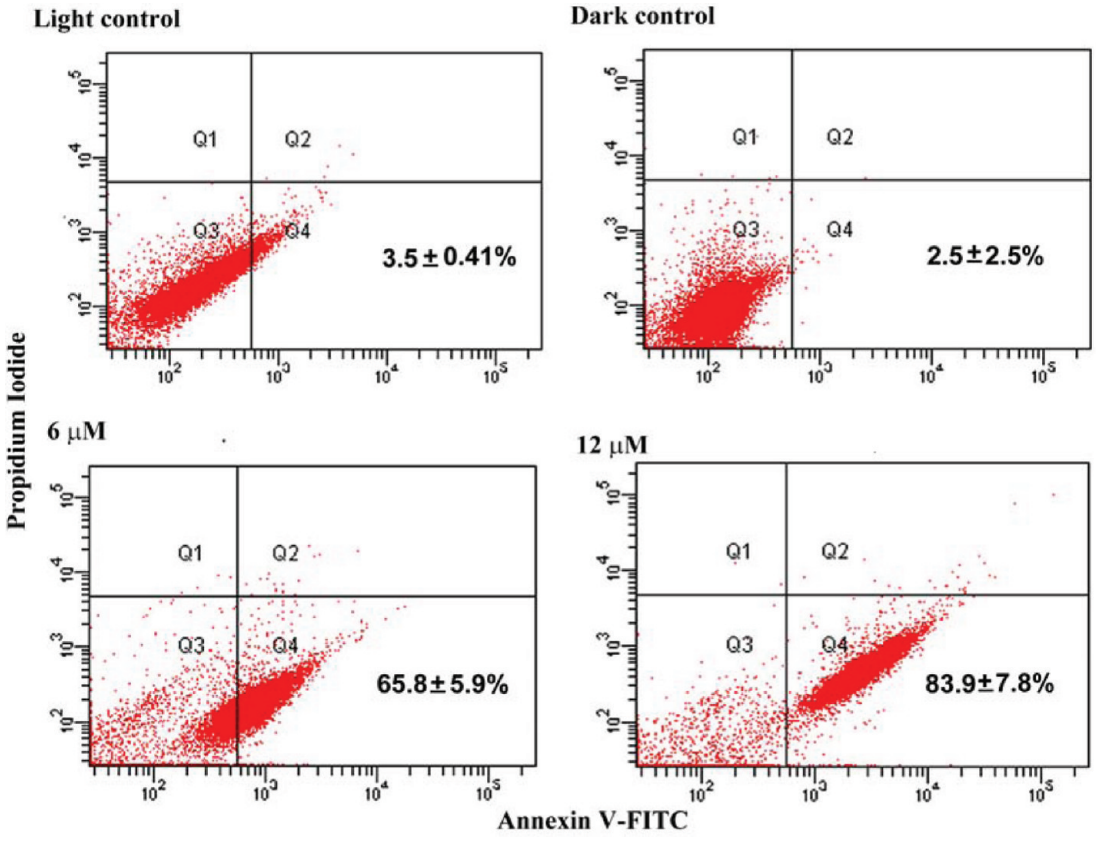

Figure 6. Flow cytometric analysis of the cell death mechanism induced by NCPS upon PDT treatment. Data are expressed as a mean value ± standard deviation of three independent experiments. The lower left quadrant (Q3) of each panel shows the viable cells, negative for both Annexin V−FITC and PI. The lower right quadrants (Q4) represent the apoptotic cells Annexin V−FITC and Propidium iodide (PI). Here, we observe an increase in apoptotic population from 3.5% ± 0.41% to 83.9% ± 7.8% when the concentration for NCPS increased from 0 to 12 μM.

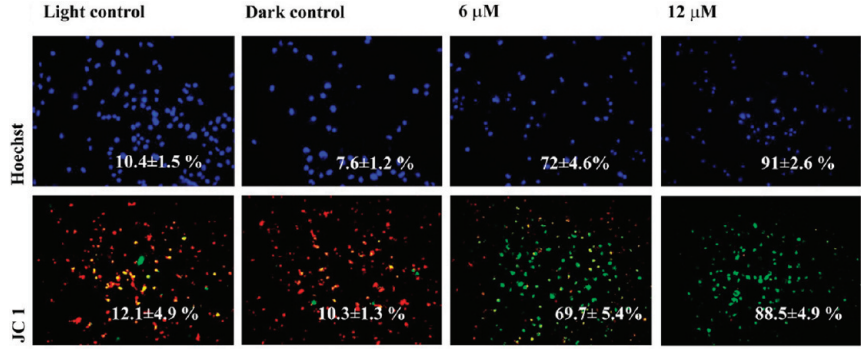

Figure 7. Characterization of cytotoxic actions of NCPS with PDT using Hoechst stain and JC1. Fluorescence cytochemistry was carried out after PDT with NCPS (6 and 12 μM). Upper panel represents Hoechst staining, and lower panel represents JC1 staining for mitochondrial membrane potential assay. In Hoechst staining, chromatin condensation was visualized using fluorescence microscope. Here apoptotic cells show peripherally clumped or condensed chromatin. In JC1 staining, cells with red color indicate healthy cells with high mitochondrial membrane potential and green color indicates apoptotic cells with low mitochondrial membrane potential.

nanosecond laser flash photolysis experiments by employing an Applied Photophysics model LKS-20 laser kinetic spectrometer using OCR-12 series Quanta Ray Nd:YAG laser. The analyzing and laser beams were fixed at right angles to each other. The laser energy was 62−66 mJ at 355 nm during the experiment. The energy transfer method to β-carotene was employed to calculate the triplet yields (Φ_T) of NCPS using $Ru(bpy)_3^{2+}$ as the reference, assuming 100% energy transfer from the reference to β-carotene. Optically matched solutions of NCPS and $Ru(bpy)_3^{2+}$ were taken at the irradiation wavelength with equal volume of a known concentration of β-carotene, where the end concentration of β-carotene was 7.48×10^{-5} M. Here, the assumption was that the transient absorbance (ΔA) of the β-carotene triplet was monitered at 520 nm for both reference and the compound, which was formed by the energy transfer from $Ru(bpy)_3^{2+}$ and NCPS triplet, respectively. The quenching of the sensitizer's triplet absorption indicates complete energy transfer to the β-carotene system. Comparison of plateau absorbance following the completion of sensitized triplet formation, properly corrected for the decay of the donor triplets in competition with energy transfer to β-carotene, enabled us to estimate Φ_T of NCPS based on the following equation:

$$\Phi_T^{comp} = \Phi_T^{ref} \frac{\Delta A^{comp}}{\Delta A^{ref}} \frac{K_{obs}^{comp}}{K_{obs}^{comp} - K_0^{comp}} \frac{K_{obs}^{ref} - K_0^{ref}}{K_{obs}^{ref}}$$

dx.doi.org/10.1021/jm300009q | J. Med. Chem. 2012, 55, 5110−5120

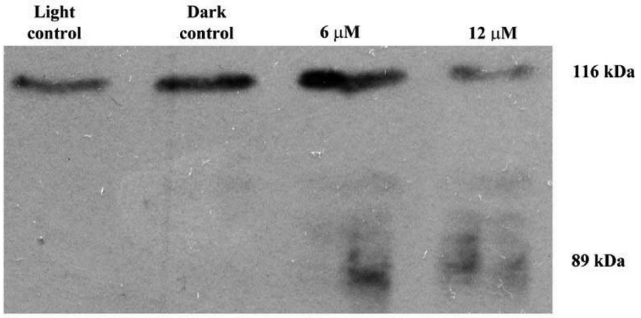

Figure 8. PARP cleavage observed after PDT with NCPS. Here there is no PARP cleavage observed in both light and dark controls, but there is significant cleavage at a concentration of 6 and 12 μM of NCPS.

Here, superscripts "comp" and "ref" can be substituted by the corresponding value of NCPS and $[Ru(bpy)_3]^{2+}$respectively. K_{obs} is the pseudo-first-order rate constant for the growth of the β-carotene triplet at 520 nm, and K_0 is the rate constant for the decay of the donor triplets at their respective triplet maximum for both the compound and reference in the absence of β-carotene. ΔA represents the plateau absorbance. The quantum yield of the reference, ruthenium−tris-bipyridine, was taken as unity in methanol.

In order to find the singlet oxygen quantum yield, a steady-state method was adopted using 1,3-diphenylisobenzofuran (DPBF) as the scavenger of singlet oxygen and *meso*-tetrakis(*p*-sulfonatophenyl)-porphyrin tetrasodium salt (TPPS) as the reference. The experiments were carried out with a light source 200 W xenon lamp (model 3767) on an Oriel optical bench (model 11200) with a grating monochromator (model 77250). The intensity of light was kept constant throughout the irradiations by measuring the output using an Oriel photodiode detection system (model 7072). Quantum yield for singlet oxygen generation of NCPS in deionized water and methanol was determined by monitoring the photooxidation of DPBF during the formation of singlet oxygen using the absorption spectrometer. Concentration of the photosensitizer was adjusted with an optical density of 0.02−0.03 at the irradiation wavelength (600 nm) to minimize the possibility of singlet oxygen quenching at higher concentration. The solution containing the sensitizer and the scavenger was purged with oxygen before irradiation. The photooxidation of DPBF was monitored with an interval of 10 s up to 1.5 min. No thermal recovery of DPBF (from a possible decomposition of endoperoxide product) was observed under the conditions of these experiments. The following equation was used to calculate the singlet oxygen quantum yield of the sensitizer with respect to the reference.

$$\Phi(^1O_2)^{comp} = \Phi(^1O_2)^{ref}\frac{m^{comp}}{m^{ref}}\frac{F^{ref}}{F^{comp}}$$

where $\Phi(^1O_2)$ is the quantum yield of singlet oxygen, superscripts "comp" and "ref" represent NCPS and TPPS, respectively, m is the slope of a plot of difference in change in absorbance of DPBF (at 411 nm) with the irradiation time, and F is the absorption correction factor, which is given by $F = 1 - 10^{-OD}$ (OD at the irradiation wavelength).

Synthesis of NCPS. To synthesize NCPS, tetraphenyl N-confused porphyrin (800 mg, 1.3 mmol) was pasted with 5 mL concentrated sulfuric acid, then transferred to a 100 mL round-bottom flask using another 15 mL of acid. The mixture was then heated at 90 °C for 5 h and then at room temperature for 12 h. Diluted sodium hydroxide solution was added slowly to the reaction mixture at 0 °C to neutralize the excess acid present. The formed sodium sulfate salt was filtered and washed many times with methanol to extract the compound. The solution was evaporated to dryness and Soxhlet extracted using methanol to obtain pure NCPS in 56% yield as greenish black solid, mp > 300 °C. ^{1}H NMR (400 MHz, DMSO-d_6): δ 8.7 (s, 1H, pyrrolic α H), 8.36 (s, 2H, pyrrolic β H), 8.28−8.29 (d, J = 3.2 Hz, 1H, pyrrolic β H), 8.25−8.26 (d, J = 3.2 Hz, 1H, pyrrolic β H), 7.86−7.88 (d, 2H, pyrrolic β H), 7.92−8.01 (m, 16H, phenyl), −1.07 (s, 1H, exch. D_2O, pyrrolic NH), −2.76 (s, 1H, pyrrolic β H). ^{13}C{^{1}H}NMR (100 MHz, DMSO-d_6): δ 167.29, 158.43, 146.18, 134.84, 134.57, 133.62, 128.82, 124.86, 124.47, 124. IR (KBr): 3448 (br), 2925, 2372, 2345, 1648, 1459, 1178, 1123, 1040 cm^{-1}. MALDI-TOF MS: m/z 1016.58 ($C_{44}H_{25}N_4Na_3O_{12}S_4 + H_2O$), 1000.98 ($C_{44}H_{27}N_4Na_3O_{12}S_4$), 936.84 ($C_{44}H_{30}N_4O_{12}S_4$ + 2H), 930.04 $(C_{44}H_{26}N_4O_{12}S_4)^{-4}$, 792.75 $(C_{44}H_{25}N_4NaO_6S_2)^{-2}$. Anal. Calcd for $C_{44}H_{26}N_4Na_4O_{12}S_4$: C, 51.66; H, 2.56; N, 5.48. Found: C, 51.01, H, 2.12, N, 5.11.

Cell Lines and Culture Conditions. Human cervical cancer cells (HeLa and SiHa), breast cancer cells (MDA-MB-231 and MCF7), colorectal cancer cells (HCT-116), and pancreatic cancer cells (MIA-PaCa-2) were purchased from ATCC (USA), and human oral cancer cells (SCC-131 and SCC-172) were obtained as a gift from Dr. Susanne M Gollin, University of Pittsburgh, USA, and were maintained in DMEM (Sigma, USA) containing 10% fetal bovine serum (Sigma, USA) and 1% antibiotic antimycotic cocktail (Invitrogen, USA). All experimental steps after seeding the cells, including photosensitizer incubation and illumination and postillumination incubation were performed in the same medium. For measurement of dark and light cytotoxicity, cells were seeded (5×10^3 per well in100 μL medium) in 96-well microplates (BD-Falcon, USA).

Photocytotoxicity Assay. NCPS was first dissolved in DMSO to give 106.9 mM solution and diluted to appropriate concentrations with the culture medium. The cells, after being rinsed with phosphate-buffered saline (PBS), were incubated with different concentration of NCPS in DMEM solutions for 1 h at 37 °C before being illuminated at an ambient temperature. A 70 W sodium vapor lamp was used as the light source with fluence rate (λ > 590 nm) of 55 mW cm^{-2}. Illumination for 30 min led to a total fluence of 100 J cm^{-2}.

Growth inhibition was determined by means of the colorimetric MTT assay. Approximately 5×10^3 cells were seeded in two 96-well cluster plates and allowed to reach the exponential phase of growth. Then NCPS was added in serial dilution at 3.34 to 53.45 μM. Out of two plates, one plate was kept in the dark for studying dark cytotoxicity. The second plate was photoirradiated using sodium vapor lamp and kept in an incubator. After illumination, the cells were incubated at 37 °C under 5% CO_2 for 24 h. MTT (Sigma Aldrich) solution in PBS (10 mg mL^{-1}, 10 μL) was added to each well followed by incubation for 4 h under the same environment. Later the media was replaced by 100 μL of isopropanol. The plate was agitated on a Bio-Rad microplate reader at ambient temperature for 10 s before the absorbance at 570 nm for each well was taken. The cell viability was then determined by the following equation: percentage growth inhibition = ({OD value of control} − {OD value of test}/{OD value of control}) × 100.

Detection of Cellular ROS Using CM-H2DCFDA Assay. For ROS stress studies, approximately 10^6 MDA-MB-231 cells were plated in 60 mm and 96-well (BD falcon) plates with serum-containing media. After 24 h, the cells were treated with 6 and 12 μM NCPS and photoirradiation was done using sodium vapor lamp for 30 min. To one plate 12 μM NCPS added and the plate was kept in dark to be taken as dark control. After 24 h of PDT with NCPS, cellular ROS content was determined using the CM-H2DCFDA probe according to the manufacturer's instructions (Invitrogen), and a flow cytometric analysis was then carried out using FACS Aria II (BD, USA). Images were taken using pathway imager (BD, USA).

Chromatin Condensation Analysis by Hoechst Staining. To study chromatin condensation, approximately 10^5 MDA-MB-231 cells were seeded in 35 mm culture dishes and incubated for 18 h. Cells were incubated with 6 and 12 μM NCPS for 1 h followed by photoirradiation using sodium vapor lamp. Light and dark control were taken as previously described. After 24 h of treatment, MDA-MB-231 cells were rinsed twice with PBS, and cells were stained with 5 μg/mL Hoechst dye 33342 (Invitrogen) for 15 min at room temperature. Cells were then washed twice with PBS and visualized under an inverted fluorescence microscope.

Mitochondrial Membrane Potential Assay Using JC1 Dye. For mitochondrial membrane potential assay, approximately 10^5 MDA-MB-231 cells were seeded in 35 mm culture dishes and incubated for 18 h. Cells were incubated with 6 and 12 μM NCPS for 1 h followed by photoirradiation using sodium vapor lamp. Light and dark control were

taken as previously described. After 24 h of treatment, MDA-MB-231 cells were rinsed twice with PBS, and cells were stained with JC1 dye mitochondrial membrane potential detection kit (Sigma Aldrich) according to the manufacturer's instruction, and the cells were examined under an inverted fluorescence microscope.

Flow Cytometric Annexin V Apoptotic Studies. Approximately 10^6 MDA-MB-231 cells were seeded on 60 mm dishes and incubated for 24 h at 37 °C under 5% CO_2. Cells were incubated with 6 and 12 μM NCPS for 1 h followed by photoirradiation using sodium vapor lamp. In this experiment, light and dark controls were taken as previously described. Cells were stained with FITC-labeled Annexin using Annexin V–FITC apoptosis detection kit (Sigma Aldrich) according to the manufacturer's instruction, and a flow cytometric analysis was then carried out using FACS Aria (BD, USA)

Immunoblot Analysis. Approximately 10^6 MDA-MB 231 cells were seeded on 60 mm dishes and incubated for 24 h at 37 °C under 5% CO_2. Cells were incubated with 6 and 12 μM NCPS for 1 h followed by photoirradiation using sodium vapor lamp. In this experiment, light and dark controls were taken as previously described. Cells were then lysed, and the total protein content was measured using Bradford's reagent. Then 50 mg of total protein was loaded for SDS–PAGE, and immunoblotting was carried out using PARP antibody (cell signaling), and horseradish peroxidase-conjugated secondary antibodies (Santa Cruz) were used, followed by detection using enhanced chemiluminescence (ECL) method.

■ ASSOCIATED CONTENT

Ⓢ Supporting Information

^{1}H and ^{13}C NMR, MALDI-TOF, and IR spectra of NCPS, fluorescence spectra of NCPS, singlet oxygen generation studies of NCPS in deionized water, and triplet decay profiles of NCPS in deionized water and methanol. This material is available free of charge via the Internet at http://pubs.acs.org.

■ AUTHOR INFORMATION

Corresponding Authors

*A. Srinivasan. Phone: +91-674-2304077. Fax: +91-674-2302436. E-mail: srini@niser.ac.in.

*M. Radhakrishna Pillai. Phone: +91-471-2347973. Fax: + 91-471-2348096. E Mail: mrpillai@rgcb.res.in.

Author Contributions

#These authors contributed equally to this work.

Notes

The authors declare no competing financial interest.

■ ACKNOWLEDGMENTS

We thank Department of Science and Technology, Govt of India (DST Grant No. SR/S5/MBD-01B/2007) and Department of Atomic Energy (DAE), India, for financial support. A.P.T. thanks CSIR, New Delhi, for a fellowship. We thank Viji, NIIST-CSIR, for MALDI-TOF, Adarsh, NIIST-CSIR, and Sanjay, NISER, for NMR analysis, and Dr. T.R. Santosh Kumar, Saneesh Varghese, and Ms. Indu Ramachandran (RGCB-DBT) for FACS analyses and imaging.

■ ABBREVIATIONS USED

NCP, N-confused porphyrin; PDT, photodynamic therapy; ROS, reactive oxygen species; FAB, fast atom bombardment; DPBF, 1,3-diphenyl isobenzofuran; DMSO-d_6, deuteriated dimethyl sulfoxide; Φ_T, triplet yields; HCT-116, human colorectal carcinoma cell; MCF-7, Michigan cancer foundation cell line; ER, estrogen receptor; PR, progesterone receptor; MDA-MB-231, M.D. Anderson metastatic breast cancer cell line; IC_{50}, dye concentration required to kill 50% of the cells; CM-H2DCFDA, 5(and 6)-chloromethyl-2′,7′-dichlorodihydofluorescein diaacetete; MIA-PaCa-2, human pancreas carcinoma from Caucasian male; SCC, squamous cell carcinoma; HeLa, Henrietta Lacks human cervical cancer cell line; SiHa, human cervical cancer cell line; MTT, 3-(4,5-dimethylthiazol-2-yl)-2,5-diphenyltetrazolium bromide; FITC, fluorescein isothiocyanate; PI, propidium iodide; JC1, (5,5′,6,6′-tetrachloro-1,1′,3,3′-tetraethylbenzimidazolylcarbocyanine iodide; PARP, poly(ADP-ribose) polymerase; DMEM, Dulbecco's modified Eagle's medium

■ REFERENCES

(1) Celli, J. P.; Spring, B. Q.; Rizvi, I.; Evans, C. L.; Samkoe, K. S.; Verma, S.; Pogue, B. W.; Hasan, T. Imaging and photodynamic therapy: Mechanisms, monitoring and optimization. *Chem. Rev.* **2010**, *110*, 2795–2838.

(2) Stockfleth, E.; Sterry, W. New treatment modalities for basal cell carcinoma. *Recent Results Cancer Res.* **2002**, *160*, 259–268.

(3) Dolmans, D. E. J. G. J.; Fukumura, D.; Jain, R. K. Photodynamic therapy for cancer. *Nat. Rev. Cancer* **2003**, *3*, 380–387.

(4) Brown, S. B.; Brown, E. A.; Walker, I. The present and future role of photodynamic therapy in cancer treatment. *Lancet Oncol.* **2004**, *5*, 497–508.

(5) Foote, C. S. Mechanisms of photosensitized oxidation. *Science* **1968**, *162*, 963–970.

(6) Lang, K.; Mosinger, J.; Wagnerovà, D. M. Photophysical properties of porphyrinoid sensitizers non-covalently bound to host molecules; models for photodynamic therapy. *Coord. Chem. Rev.* **2004**, *248*, 321–350.

(7) Sol, V.; Blais, J. C.; Carré, V.; Granet, R.; Guilloton, M.; Spiro, M.; Krausz, P. Synthesis, spectroscopy, and photocytotoxicity of glycosylated amino acid porphyrin derivatives as promising molecules for cancer phototherapy. *J. Org. Chem.* **1999**, *64*, 4431–4444.

(8) Regehly, M.; Greish, K.; Rancan, F.; Maeda, H.; Böhm, F.; Röder, B. Water-soluble polymer conjugates of ZnPP for photodynamic tumor therapy. *Bioconjugate Chem.* **2007**, *18*, 494–499.

(9) Sternberg, E. D.; Dolphin, D.; Brückner, C. Porphyrin-based photosensitizers for use in photodynamic therapy. *Tetrahedron* **1998**, *54*, 4151–4202.

(10) Kessel, D.; Thompson, P.; Saatio, K.; Nantwi, K. D. Tumor localization and phosensitization by sulfonated derivatives of tetraphenylporphine. *Photochem. Photobiol.* **1987**, *45*, 787–790.

(11) Grebeová, D.; Cajthamlová, H.; Holada, K.; Marinov, J.; Jirsa, M.; Hrkal, Z. Photodynamic effects of *meso*-tetra(4-sulfonatophenyl)-porphine on human leukemia cells HEL and HL6, human lymphocytes and bone marrow progenitor cells. *J. Photochem. Photobiol., B* **1997**, *39*, 269–278.

(12) Wainwright, M. Non-porphyrin sensitizers in biomedicine. *Chem. Soc. Rev.* **1996**, *25*, 351–359.

(13) Kadish, K. M.; Smith, K. M.; Guilard, R. *The Porphyrin Handbook*; Academic Press: San Diego, CA, 2000; Vol. *VI*, Chapters 40–46.

(14) Detty, M. R.; Gibson, S. L.; Wagner, S. J. Current clinical and preclinical photosensitizers for use in photodynamic therapy. *J. Med. Chem.* **2004**, *47*, 3897–3915.

(15) Rosenthal, D. I.; Nurenberg, P.; Becerra, C. R.; Frenkel, E. P.; Carbone, D. P.; Lum, B. L.; Miller, R.; Engel, J.; Young, S.; Miles, D. A phase I single-dose trial of gadolinium texaphyrin (Gd-Tex), a tumor selective radiation sensitizer detectable by magnetic resonance imaging. *Clin. Cancer Res.* **1999**, *5*, 739–745.

(16) Arnbjerg, J.; Jiménez-Banzo, A.; Paterson, M. J.; Nonell, S.; Borrell, J. I.; Christiansen, O.; Ogilby, P. R. Two-photon absorption in tetraphenylporphycenes: Are porphycenes better candidates than porphyrins for providing optimal optical properties for two-photon photodynamic therapy? *J. Am. Chem. Soc.* **2007**, *129*, 5188–5199.

(17) Ethirajan, M.; Chen, Y.; Joshy., P.; Pandey, R. K. The role of porphyrin chemistry in tumour imaging and photodynamic therapy. *Chem. Soc. Rev.* **2011**, *40*, 340–362.

(18) Bonnett, R. *Chemical Aspects of Photodynamic Therapy*; CRC: Boca Raton, FL, 2000; Vol. *1*.
(19) Dougherty, T. J.; Gomer, C. J.; Henderson, B. W.; Jori, G.; Kessel, D.; Korbelik, M; Moan, J.; Peng, Q. Photodynamic therapy: Review. *J. Natl. Cancer Inst.* **1998**, *90*, 889−902.
(20) Furuta, H.; Asano, T.; Ogawa, T. "N-Confused porphyrin": A new isomer of tetraphenylporphyrin. *J. Am. Chem. Soc.* **1994**, *116*, 767−768.
(21) Chmielewski, P. J.; Latos-Grażyński, L.; Rachlewicz, K.; Glowiak, T. Tetra-*p*-tolylporphyrin with an inverted pyrrole ring: A novel isomer of porphyrin. *Angew. Chem., Int. Ed. Engl.* **1994**, *33*, 779−781.
(22) Xie, Y.; Morimoto, T.; Furuta, H. Sn^{IV} complexes of N-confused porphyrins and oxoporphyrins—unique fluorescence "switch on" halide receptors. *Angew. Chem., Int. Ed.* **2006**, *45*, 6907−6910.
(23) Modzianowska, A.; Latos-Grażyński, L.; Szterenberg, L.; Stępień, M. Single-boron complexes of N-confused and N-fused porphyrins. *Inorg. Chem.* **2007**, *46*, 6950−6957.
(24) Sripothongnak, S.; Ziegler, C. J. Lithium complexes of N-confused porphyrin. *Inorg. Chem.* **2010**, *49*, 5789−5791.
(25) Zhu, X.; Wong, W. K.; Lo, W. K.; Wong, W. Y. Synthesis and crystal structure of the first lanthanide complex of *N*-confused porphyrin with an η^2 agostic C−H interaction. *Chem. Commun.* **2005**, 1022−1024.
(26) Harvey, J. D.; Ziegler, C. J. Developments in the metal chemistry of N-confused porphyrin. *Coord. Chem. Rev.* **2003**, *247*, 1−19.
(27) Chmielewski, P. J.; Latos-Grażyński, L. Core modified porphyrins-a macrocyclic platform for organometallic chemistry. *Coord. Chem. Rev.* **2005**, *249*, 2510−2533.
(28) Srinivasan, A.; Furuta, H. Confusion approach to porphyrinoid chemistry. *Acc. Chem. Res.* **2005**, *38*, 10−20.
(29) Srinivasan, A.; Toganoh, M.; Niino, T.; Osuka, A.; Furuta, H. Synthesis of N-confused tetraphenylporphyrin rhodium complexes having versatile metal oxidation states. *Inorg. Chem.* **2008**, *47*, 11305−11313.
(30) Maeda, H.; Morimoto, T.; Osuka, A.; Furuta, H. Halide-anion binding by singly and doubly N-confused porphyrins. *Chem.—Asian J.* **2006**, *1*, 832−844.
(31) Ikawa, Y.; Moriyama, S.; Harada, H.; Furuta, H. Acid−base properties and DNA-binding of water soluble N-confused porphyrins with cationic side-arms. *Org. Biomol. Chem.* **2008**, *6*, 4157−4166.
(32) Ikawa, Y.; Ogawa, H.; Harada, H.; Furuta, H. N-confused porphyrin possessing glucamine-appendants: Aggregation and acid/base properties in aqueous media. *Bioorg. Med. Chem. Lett.* **2008**, *18*, 6394−6397.
(33) Du, Y.; Zhang, D.; Chen, W.; Zhang, M.; Zhou, Y.; Zhou, X. Cationic N-confused porphyrin derivative as a better molecule scaffold for G-quadruplex recognition. *Bioorg. Med. Chem.* **2010**, *18*, 1111−1116.
(34) Geier, G. R., III; Haynes, D. M.; Lindsey, J. S. An efficient one-flask synthesis of N-confused tetraphenylporphyrin. *Org. Lett.* **1999**, *1*, 1455−1458.
(35) Krishnamurthy, M. Kinetics of anation reactions of a water-soluble Rh(III)-porphyrin. *Inorg. Chim. Acta* **1977**, *25*, 215−218.
(36) See the Supporting Information.
(37) Belair, J. P.; Ziegler, C. J.; Rajesh, C. S.; Modarelli, D. A. Photophysical characterization of free-base N-confused tetraphenylporphyrins. *J. Phys. Chem. A* **2002**, *106*, 6445−6451.
(38) Engelmann, F. M.; Mayer, I.; Araki, K.; Toma, H. E.; Baptista, M. S.; Maeda, H.; Osuka, A.; Furuta, H. Photochemistry of doubly N-confused porphyrin bonded to non-conventional high oxidation state Ag(III) and Cu(III) ions. *J. Photochem. Photobiol., A* **2004**, *163*, 403−411.
(39) Ryu, J. H.; Ito, F.; Nagamura, T.; Nakamura, K.; Furuta, H.; Shibata, Y.; Itoh, S. Excited-state dynamics of normal and doubly N-confused type hexaphyrin derivatives studied by time-resolved fluorescence measurements. *Chem. Phys. Lett.* **2007**, *443*, 274−279.
(40) Kwon, J. H.; Ahn, T. K.; Yoon, M.; Kim, D. Y.; Koh, M. K.; Kim, D. Comparative photophysical properties of free-base, bis-Zn(II), bis-Cu(II), and bis-Co(II) doubly N-confused hexaphyrins(1.1.1.1.1.1). *J. Phys. Chem. B* **2006**, *110*, 11683−11690.
(41) Kumar, C. V.; Qin, L.; Das, P. K. Aromatic thioketone triplets and their quenching behaviour towards oxygen and di-t-butylnitroxy radical. A laser-flash-photolysis study. *J. Chem. Soc., Faraday Trans. 2* **1984**, *80*, 783−793.
(42) Ramaiah, D.; Joy, A.; Chandrasekhar, N.; Eldho, N. V.; Das, S.; George, M. V. Halogenated squaraine dyes as potential photochemotherapeutic agents. synthesis and study of photophysical properties and quantum efficiencies of singlet oxygen generation. *Photochem. Photobiol.* **1997**, *65*, 783−790.
(43) Rossi, L. M.; Silva, P. R.; Vono, L. L. R.; Fernandes, A. U.; Tada, D. B.; Baptista, M. S. Protoporphyrin IX nanoparticle carrier: Preparation, optical properties, and singlet oxygen generation. *Langmuir* **2008**, *24*, 12534−12538.
(44) Adarsh, N.; Avirah, R. R.; Ramaiah, D. Tuning photosensitized singlet oxygen generation efficiency of novel aza-BODIPY dyes. *Org. Lett.* **2010**, *12*, 5720−5723.
(45) Jiang, X. J.; Yeung, S. L.; Lo, P. C.; Fong, W. P.; Ng, D. K. P. Phthalocyanine−polyamine conjugates as highly efficient photosensitizers for photodynamic therapy. *J. Med. Chem.* **2011**, *54*, 320−330.
(46) Wilkinson, F.; Helman, W. P.; Ross, A. B. Quantum yields for the photosensitized formation of the lowest electronically excited singlet state of molecular oxygen in solution. *J. Phys. Chem. Ref. Data* **1993**, *22*, 113−262.
(47) Tanielian, C.; Wolff, C.; Esch, M. Singlet oxygen production in water: Aggregation and charge-transfer effects. *J. Phys. Chem.* **1996**, *100*, 6555−6560.
(48) Grebeňová, D.; Cajthamlová, H.; Holada, K.; Marinov, J.; Jirsa, M.; Hrkal, Z. Photodynamic effects of meso-tetra(4-sulfonatophenyl)-porphine on human leukemia cells HEL and HL60, human lymphocytes and bone marrow progenitor cells. *J. Photochem. Photobiol,. B* **1997**, *39*, 269−278.
(49) Stilts, C. E.; Nelen, M. I.; Hilmey, D. G.; Davies, S. R.; Gollnick, S. O.; Oseroff, A. R.; Gibson, S. L.; Hilf, R.; Detty, M. R. Water soluble, core-modified porphyrins as novel, longer-wavelength absorbing sensitizers for photodynamic therapy. *J. Med. Chem.* **2000**, *43*, 2403−2410.
(50) Van Lier, J. E.; Tian, H.; Ali, H.; Cauchon, N.; Hassèssian, H. M. Trisulfonated porphyrazines: New photosensitizers for the treatment of retinal and subretinal edema. *J. Med. Chem.* **2009**, *52*, 4107−4110.
(51) Fuchs, J.; Thiele, J. The role of oxygen in cutaneous photodynamic therapy. *Free Radical Biol. Med.* **1998**, *24*, 835−847.
(52) Wang, Y.; He, Q. Y.; Sun, R. W. Y.; Che, C. M.; Chiu, J. F. Gold (III) porphyrin 1a induced apoptosis by mitochondrial death pathways related to reactive oxygen species. *Cancer. Res.* **2005**, *65*, 11553−11564.
(53) Josefsen, L. B.; Boyle, R. W. Photodynamic therapy and the development of metal-based photosensitisers. *Met.-Based Drugs* **2008**, *2008*, 1−24.
(54) Kiesslich, T.; Krammer, B.; Plaetzer, K. Cellular mechanisms and prospective applications of hypericin in photodynamic therapy. *Curr. Med. Chem.* **2006**, *13*, 2189−2204.
(55) Mroz, P.; Bhaumik, J.; Dogutan, D. K.; Aly, Z.; Kamal, Z.; Khalid, L.; Kee, H. L.; Bocian, D. F.; Holten, D.; Lindsey, J. S. Imidazole metalloporphyrins as photosensitizers for photodynamic therapy: Role of molecular charge, central metal and hydroxyl radical production. *Cancer Lett.* **2009**, *282*, 63−76.
(56) Rapozzi, V.; Umezawa, K.; Xodo, L. E. Role of NF B/Snail/RKIP loop in the response of tumor cells to photodynamic therapy. *Laser Surg. Med.* **2011**, *43*, 575−585.
(57) Usuda, J.; Chiu, S. M; Azizuddin, K.; Xue, L. Y.; Lam, M.; Nieminen, A. L.; Oleinick, N. L. Promotion of photodynamic therapy-induced apoptosis by the mitochondrial protein Smac/DIABLO: Dependence on Bax. *Photochem. Photobiol.* **2002**, *76*, 217−223.
(58) Thompson, H. J.; Strange, R.; Schedin, P. J. Apoptosis in the genesis and prevention of cancer. *Cancer Epidemiol. Biomarkers Prevent.* **1992**, *1*, 597−602.
(59) Oleinick, N. L.; Morris, R. L.; Belichenko, I. The role of apoptosis in response to photodynamic therapy: What, where, why, and how. *Photochem. Photobiol. Sci.* **2002**, *1*, 1−21.
(60) Vermes, I.; Haanen, C.; Steffens-Nakken, H.; Reutellingsperger, C. A novel assay for apoptosis flow cytometric detection of

phosphatidylserine expression on early apoptotic cells using fluorescein labelled annexin V. *J. Immunol. Methods* **1995**, *184*, 39−51.
(61) Compton, M. M. A biochemical hallmark of apoptosis: Internucleosomal degradation of the genome. *Cancer. Metastasis Rev.* **1992**, *11*, 105−119.
(62) Liu, X.; Li, P.; Widlak, P.; Zou, H.; Luo, X.; Garrard, W. T.; Wang, X. The 40-kDa subunit of DNA fragmentation factor induces DNA fragmentation and chromatin condensation during apoptosis. *Proc. Natl. Acad. Sci. U.S.A.* **1998**, *95*, 8461−8466.
(63) Saraste, A.; Pulkki, K. Morphologic and biochemical hallmarks of apoptosis. *Cardiovasc. Res.* **2000**, *45*, 528−537.
(64) Lemasters, J. J.; Qian, T.; He, L.; Kim, J. S.; Elmore, S. P.; Cascio, W. E.; Brenner, D. A. Role of mitochondrial inner membrane permeabilization in necrotic cell death, apoptosis, and autophagy. *Antioxid. Redox Signaling* **2002**, *4*, 769−781.
(65) Castedo, M.; Hirsch, T.; Susin, S. A.; Zamzami, N.; Marchetti, P.; Macho, A.; Kroemer, G. Sequential acquisition of mitochondrial and plasma membrane alterations during early lymphocyte apoptosis. *J. Immunol.* **1996**, *157*, 512−521.
(66) Kirshner, J. R.; He, S.; Balasubramanyam, V.; Kepros, J.; Yang, C. Y.; Zhang, M.; Du, Z.; Barsoum, J.; Bertin, J. Elesclomol induces cancer cell apoptosis through oxidative stress. *Mol. Cancer Ther.* **2008**, *7*, 2319−2327.
(67) Mathur, A.; Hong, Y.; Kemp, B. K.; Barrientos, A. A.; Erusalimsky, J. D. Evaluation of fluorescent dyes for the detection of mitochondrial membrane potential changes in cultured cardiomyocytes. *Cardiovasc. Res.* **2000**, *46*, 126−138.
(68) Bernardi, P.; Scorrano, L.; Colonna, R.; Petronilli, V.; Di Lisa, F. Mitochondria and cell death. Mechanistic aspects and methodological issues. *Eur. J. Biochem.* **1999**, *264*, 687−701.
(69) Satoh, M. S.; Lindahl, T. Role of poly (ADP-ribose) formation in DNA repair. *Nature* **1992**, *356* (6367), 356−358.
(70) Lazebnik, Y. A; Kaufmann, S. H; Desnoyers, S.; Poirier, G. G.; Earnshaw, W. C. Cleavage of poly (ADP-ribose) polymerase by a proteinase with properties like ICE. *Nature* **1994**, *371* (6495), 346−347.
(71) Cohen, G. M. Caspases: The executioners of apoptosis. *Biochem. J.* **1997**, *326*, 1−16.
(72) Nicholson, D. W.; Ali, A.; Thornberry, N. A.; Vaillancourt, J. P.; Ding, C. K.; Gallant, M.; Gareau, Y.; Griffin, P. R.; Labelle, M.; Lazebnik, Y. A. Identification and inhibition of the ICE/CED-3 protease necessary for mammalian apoptosis. *Nature* **1995**, *376* (6535), 37−43.
(73) Tewari, M.; Quan, L. T.; O'Rourke, K.; Desnoyers, S.; Zeng, Z.; Beidler, D. R.; Poirier, G. G.; Salvesen, G. S.; Dixit, V. M. Yama/CPP32 [beta], a mammalian homolog of CED-3, is a CrmA-inhibitable protease that cleaves the death substrate poly (ADP-ribose) polymerase. *Cell* **1995**, *81*, 801−809.
(74) Oliver, F. J.; de la Rubia, G.; Rolli, V.; Ruiz-Ruiz, M. C.; de Murcia, G.; Murcia, J. M. Importance of poly (ADP-ribose) polymerase and its cleavage in apoptosis. *J. Biol. Chem.* **1998**, *273*, 33533−33539.